

PAPER • OPEN ACCESS

## The analysis of the dimple arrangement of the artificial hip joint to the performance of lubrication

To cite this article: Hasan Basri *et al* 2019 *IOP Conf. Ser.: Mater. Sci. Eng.* **620** 012116

View the [article online](#) for updates and enhancements.

### Recent citations

- [The Effect of Bottom Profile Dimples on the Femoral Head on Wear in Metal-on-Metal Total Hip Arthroplasty](#)  
J. Jamari *et al*
- [The Effect of Texture Floor Profile on the Lubricant Film Thickness in a Textured Hard-On-Soft Bearing With Relevance to Prosthetic Hip Implants](#)  
Quentin Allen and Bart Raeymaekers
- [Maximizing the Lubricant Film Thickness Between a Rigid Microtextured and a Smooth Deformable Surface in Relative Motion, Using a Soft Elasto-Hydrodynamic Lubrication Model](#)  
Bart Raeymaekers and Quentin Allen



**ECS** **240th ECS Meeting**  
Digital Meeting, Oct 10-14, 2021

**Register early and save up to 20% on registration costs**

Early registration deadline Sep 13

**REGISTER NOW**

# The analysis of the dimple arrangement of the artificial hip joint to the performance of lubrication

Hasan Basri<sup>1,\*</sup>, A Syahrom<sup>2,3</sup>, T S Ramadhoni<sup>1</sup>, A T Prakoso<sup>1</sup>,  
M. I. Ammarullah<sup>1</sup>, Vincent<sup>1</sup>

<sup>1</sup> Department of Mechanical Engineering, Faculty of Engineering, Universitas Sriwijaya, Indralaya, 30662, Kabupaten Ogan Ilir.

<sup>2</sup> Department of Applied Mechanics and Design, Faculty of Mechanical Engineering, Universiti Teknologi Malaysia, Skudai 81310, Johor, Malaysia.

<sup>3</sup> Sports Innovation and Technology Centre (SITC), Institute of Human-Centred and Engineering (IHCE).

\*hasan\_basri@unsri.ac.id

**Abstract.** Artificial hip joint surgery is one of the most successful methods used to restore the functioning of damaged hip bones. But there are obstacles to the use of artificial hip bone, which is the amount of friction occurring and wears. To overcome these obstacles, a surface of the artificial hip joint is modified by adding dimples in order to minimize the contact pressure of solid and to reduce friction and wear. The purpose of this study is to determine a better of lubrication performance with the variations of the dimple arrangements under the normal walking condition. Simulation results have already exited the point of convergence studies, and the obtained results are such as hydrodynamic pressure, contact pressure, and the film thickness of the lubricant with the variations of the number and pitch dimples. The results of the CSM method under dry condition, it shows that the addition of surface with dimples has a positive effect to reduce the contact pressure and indirectly reduce wear. The maximum surface contact pressure is 54.84 MPa with dimple and 94.22 MPa without a dimple. The results of the FSI method under lubrication condition, it was found that the variation of 7 dimples with a dimple pitch of 500  $\mu\text{m}$  has the best lubrication performance. The hydrodynamic pressure is 0.73 Pa, the contact pressure is 0.42 Pa, and the film thickness of the lubricant is 29.59  $\mu\text{m}$ . The increase of film thickness that occurs due to hydrodynamic pressure will cause the fluid lift force to withstand the loading of the solid structure.

**Keywords:** surface texturing, lubrication performance, artificial hip joint, fluid-structure interaction, dimple

## 1. Introduction

Total Hip Arthroplasty (THA) is one of joint replacement surgery that successful in the world of orthopedic surgery [1]. THA can replace the damage, pain release and fix or improve range of motion of hip joint [1,2]. Recently, the most used material for THA is Metal-on-Metal (MoM) and Metal-on-Polyethylene (MoP) [3]. MoM material was attracting many researchers [4,5] to focus on due to their most successful in term of survival rate in an average 74% (28 years) [6]. While MoP prostheses cause aseptic loosening that limiting the longevity and, being associated with the release of polyethylene wear particles. Whereas there is still the disadvantage of MoM like the local effect of metal particles



after revision surgery [2,7]. The increased of Co ions concentrations in patients that have MoM prostheses are a concern since increased Co ions levels in blood [8,9], cardiac (myocardiopathy) [10,11] and endocrine (aberrant estrogen signaling, altered the production or circulation of sex hormones, and altered thyroid metabolism) [8,12] symptoms.

Most researchers focused on reducing wear debris, improved range of motion and a lower dislocation rate with prostheses design and improve quality surface technique [4,13]. MoM prostheses can have a larger diameter, increasing joint stability, which is associated with a lower long-term risk of dislocation so that the incidence of THA is lower [6]. Prosthetic wear in MoM reported being 60 times less than expected with conventional MoP prostheses [5]. Therefore, the larger femoral head is a major concern for greater volumetric wear. However, surface texturing was suggested by the previous study [5,14,15] to reduce wear, increase film thickness and therefore increase the lifetime of a MoM prosthesis.

Surface texturing is widely used in mechanics to increase the load carrying capacity of various kinds of joints in working lubrication condition [16]. Furthermore, it had been proposed to increase the tribological performance of hip prostheses. Some improvements can be seen in the literature related to different surface textures of hip joints. The previous study reported using a dimpled surface such as spherical [17], well-defined honed [18,19], and cylinder shape was shown to improve tribological performance is reducing friction and wear, and increasing hydrodynamic pressure lift. However, the effect of surface texturing on the tribological performance improvements dependent on a geometrical parameter such as shape, diameter, density, depth and pitch of dimples [20]. To improve lubrication performance, optimization of geometric surface texture designs has been carried out experimentally [17–19,21–23], numerical analysis [17–19,24–28] and computational fluid dynamics [29,30].

In this study, we modify the contact area on the acetabular liner by adding dimples in order to minimize the contact pressure of solids and to reduce friction and wear in the performance of lubricating on the artificial hip joint by the Computational Solid Mechanics (CSM) method and the Fluid-Structure Interaction (FSI) method using COMSOL Multiphysics 4.3b software.

The purpose of this study was to obtain the optimum geometry of the dimple in order to improve tribological performance, especially from a lubrication using the Fluid-Structure Interaction (FSI) method. The research method focused on the numerical analysis of the 2D Finite Element Method (FEM) using Computational Solid Mechanic (CSM) which reviewed the solid and solid structure and Fluid-Structure Interaction (FSI) simulation method which reviewed the solid and fluid structure.

## 2. Materials and Method

### 2.1. Material and dimensions

The main components of the model were assumed homogeneous and linear elastic isotropic. CoCrMo material properties derived from the literature [31–33], therefore the modulus of elasticity, Poisson ratio, and material density are 210 GPa, 0.3, and 8300 kg/m<sup>3</sup> respectively. The dimension of acetabular cup (RC) and femoral head radius (RH) was 23.5 mm and 14 mm respectively. Basically, the range of movement of the femoral head around the x, y, and z-direction represented the adduction-abduction, internal-external rotation, and flexion-extension motion, respectively. Figure 1b shows the cross-sectional view of YZ direction, including multiple dimpled surfaces. The radial clearance between the cup and head was 30  $\mu$ m. This 2D model was used to analyze the lubrication performance of dimpled surfaces as shown in Figure 1c. The model of parallel plates was considered to investigate the effects of geometric parameters of dimpled surfaces. The parallel plate length, width, clearance, dimple diameter, and dimple depth are denoted by the symbols L, R, Ho, D, and H, respectively.

### 2.2. Modeling

The design of the model used in Comsol Multiphysics 4.3b is a 2D ball and cup model that has a dimple and without dimple in a non-lubricated condition that will be simulated with computational solid mechanics (CSM) completion. The dimension of acetabular cup radial clearance (RC) and

femoral head radius (HR) was 23.5 mm and 14 mm respectively. Basically, the range of movement of the femoral head around the x, y, and z-direction represented the adduction-abduction, internal-external rotation, and flexion-extension motion, respectively. Figure 1b shows the cross-sectional view of YZ direction, including multiple dimpled surfaces. Then, the second model is a sample of the artificial hip joint component in the form of two plates representing the femoral head and acetabular cup, of which one plate is given dimple with varying amount of dimple and pitch dimple under lubrication conditions which will be simulated with the completion of FSI.

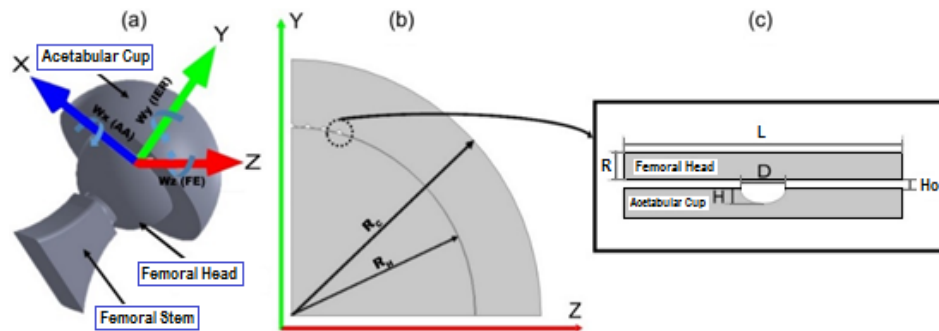


**Figure 1.** (a) Model of hip joint prostheses; (b) cross-section view of YZ direction; and (c) sectional view of the dimpled surface.

### 2.2.1. Modeling of 2D ball and cup

The model is made in the form of a quarter circle because the model is assumed to be symmetrical as shown in Figure 2a.

### 2.2.2. Two plates model variations

Modeling on these 2D plates can be assumed to represent the sample of the dimple in the ball and cup modeling. This modeling is varied into 9 variants that will represent from 3 types of many numbers of the dimple and 3 types of pitch dimple. The number of dimples used is 3 dimples, 5 dimples, and 7 dimples and the pitch of dimples are 100  $\mu\text{m}$ , 300  $\mu\text{m}$  and 500  $\mu\text{m}$  as shown in Figure 3. The elliptical dimension geometry is 150  $\mu\text{m}$  diameters and a depth of 37.5  $\mu\text{m}$  that are taken into the shape of the dimple because it has a good lubrication performance based on previous research by [35,36]. The dimple and without dimple models for these two plates are shown in Figure 2b.

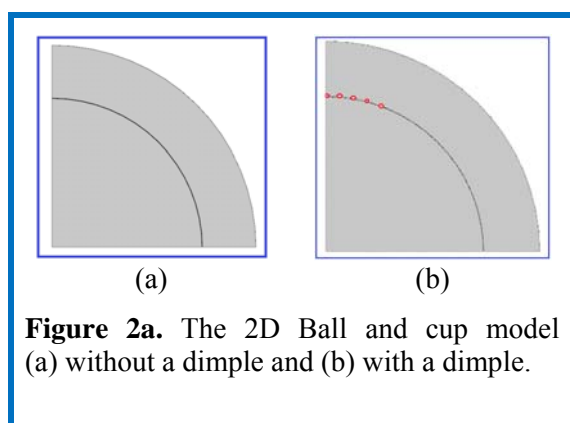


**Figure 2a.** The 2D Ball and cup model (a) without a dimple and (b) with a dimple.

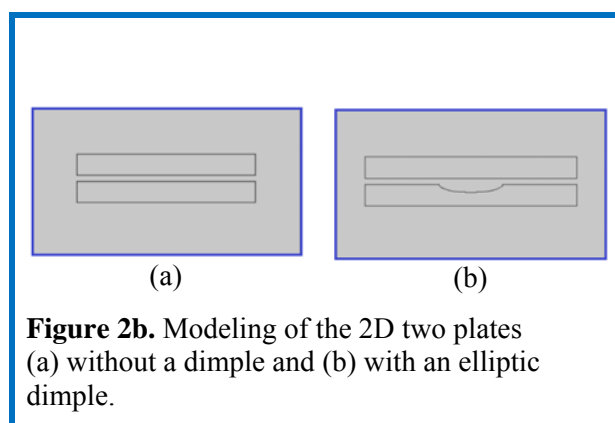


**Figure 2b.** Modeling of the 2D two plates (a) without a dimple and (b) with an elliptic dimple.

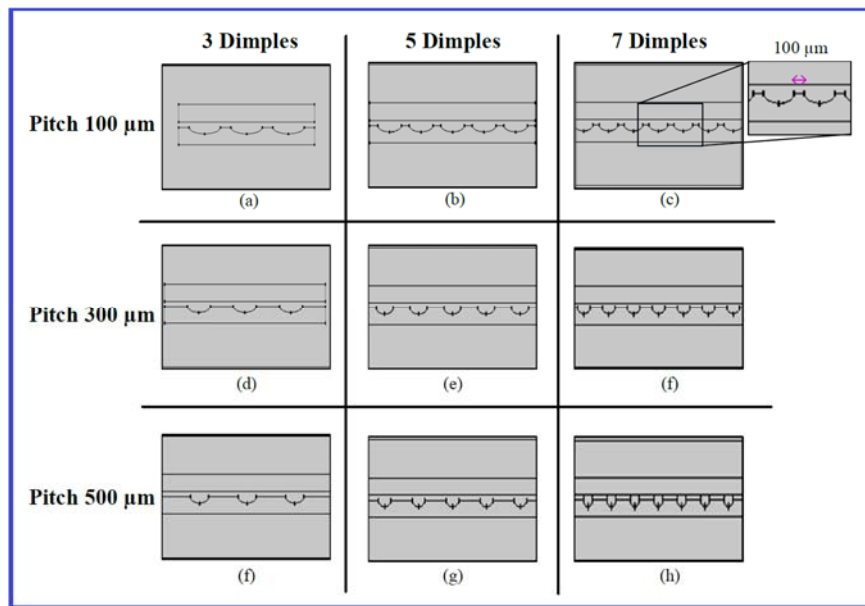


**Figure 3.** Modeling of the 2D two plates with an elliptic dimple.

### 2.3. Boundary condition model for simulation

The boundary condition of the model is shown in Figure 4a. The acetabular cup was fixed constraint as shown in Figure 4a as the same as a previous work [34]. The load was given on the upper side of the femoral head based on physiological loading condition (normal walking) using dynamic load and motion profiles taken which refer to standard ISO 14242-1 as shown in Figure 4b. The gap between the two plates is denoted as  $H_0$  representing the film thickness of the lubricant with a constant initial value of  $30\ \mu\text{m}$ . During the FSI simulation procedure, the mesh sensitivity analysis of dimpled surface was conducted to determine the optimum mesh size.

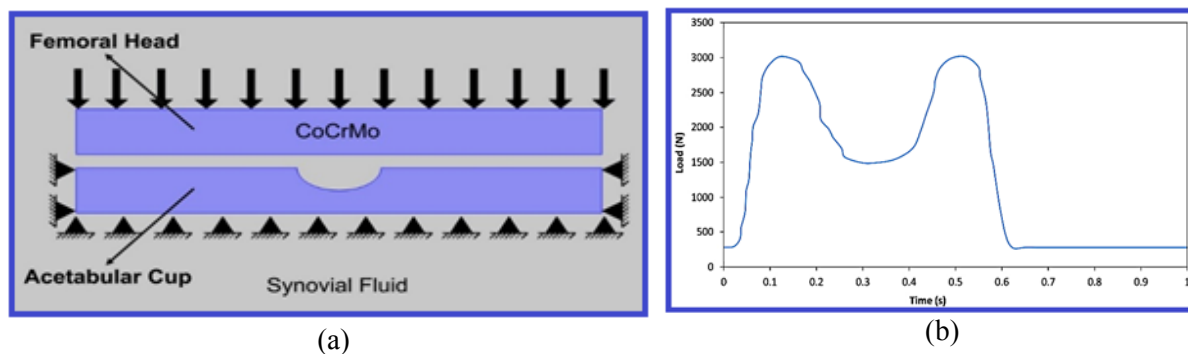


**Figure 4.** (a) The boundary condition of the FSI model (b) Loading profile on normal gait walking condition [24].

Lubrication performance of dimpled surfaces was analyzed using computational simulation FSI of commercial software Comsol Multiphysics 4.3b, USA. This simulation was solved using time-dependent condition that has a range of 0 to 1 second with a time step of 0.01 second. The entire domain of the model is filled in by a synovial fluid as a lubricant with the no-slip condition on each side wall. The lubricant was assumed as Newtonian fluid, incompressible, and isoviscous. The lubricant properties such as dynamic viscosity and fluid density are  $0.0025\ \text{Pa}$  and  $1012\ \text{kg/m}^3$ , respectively [32,33].

#### 2.4. Meshing model

The meshing model applied to the completion of the model, should first be done in convergence studies (mesh sensitivity). This convergence study is very important to reduce the time to complete the finite element model and it will get an effective mesh of the model.

##### 2.4.1 Meshing sensitivity model of ball and cup

The meshing model of the 2D ball and the cup as shown in Figure 5a and the meshing models in the numerical simulation shown in Figure 5b. Based on the analysis of mesh sensitivity, the result of the 2D ball and the cup meshing, the model is divided into 5 mesh types. Identification of meshing sensitivity is intended to predict the parameters of a contact between acetabular cup and femoral head. The contact pressure is selected as a parameter to identify the best meshing. Figure 6 shows the selected meshing at 94.216 MPa contact pressure with a total of 5784 elements.

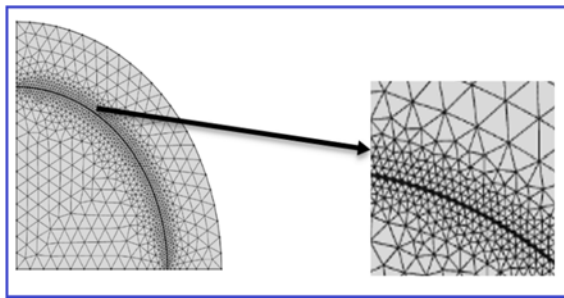


**Figure 5a.** Example of meshing on the 2D modeling ball in the socket.

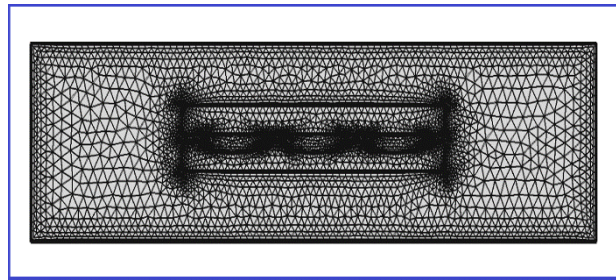


**Figure 5b.** Detail meshing of 2D models in numerical simulation.

##### 2.4.2. Meshing sensitivity of two plates model

Based on the analysis of mesh sensitivity, the results of the 2D meshing, the model can be divided into 7 mesh types. The identification of meshing sensitivity is thought to predict the parameters of the lubrication occurring on two plates representing the lubrication between acetabular cup and femoral head. The velocity of the fluid is used as a parameter to identify the best meshing as it has a stable value for analysis. The velocity value of the analysis had to be independent of element numbers, where the hydrodynamic pressure directly dependent on the velocity. Figure 7 shows the selected meshing at the fluid velocity of  $7.18 \times 10^{-5}$  m/s with the number of 360442 elements.

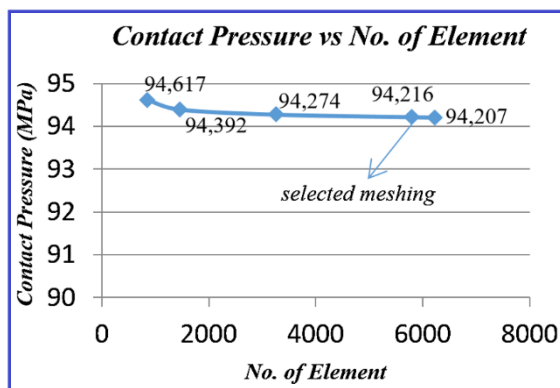


**Figure 6.** The relationship between contact pressure and the number of elements.

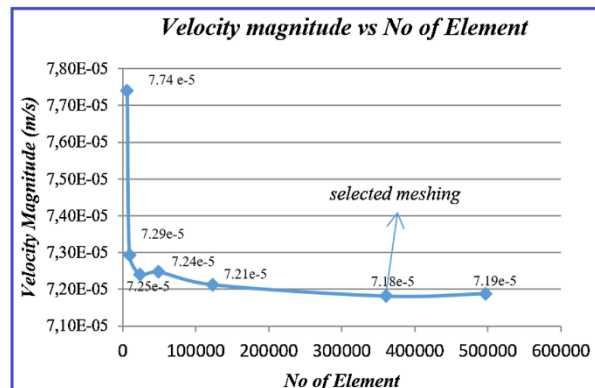


**Figure 7.** The relationship between fluid velocity and the number of elements.

### 3. Results and discussion

The result of ball and cup modeling using CSM is the contact pressure. Based on Figure 8, we can see the value of contact pressure to the coordinate angle where the contact pressure between surfaces without dimple with the Hertz theory approach almost the same. This is evidence that by the maximum value of surface contact pressure without dimple is 94.216 MPa, while the upper limit value of the contact pressure of the Hertz theory is 89.6 MPa. As for the result of contact pressure on the surface with a dimple, the maximum contact pressure is only 54.84 MPa. The smaller contact pressure with the addition of dimple becomes the foundation for the next research stage of the FSI method under lubrication conditions.

From Figure 9, it can be seen that the hydrodynamic pressure on the surface of the dimple is greater than without a dimple. This is indicated by the value of the hydrodynamic pressure at the loading time of 0.12 seconds for the dimple surface is 0.702 Pa and the surface without dimple is 0.657 Pa. Greater hydrodynamic pressures provide a positive effect to improve the lubrication performance because increased in hydrodynamic pressure also affects the increase in lubricating film thickness film. The greater the hydrodynamic pressure of the fluid on the surface is in accordance with the research done by [29,36].

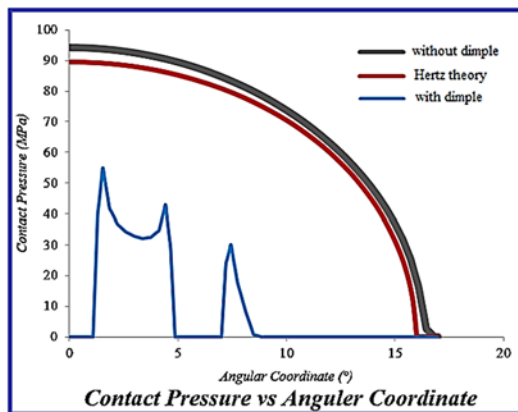


**Figure 8.** Comparison of contact pressure of ball and cup in dry contact condition.

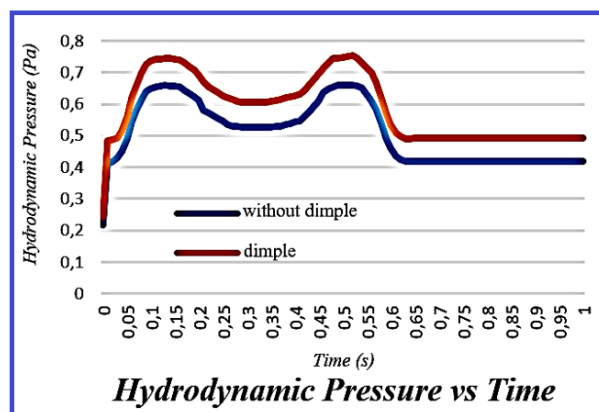


**Figure 9.** Comparison of hydrodynamic pressure ratio on the surface of the dimple and without a dimple.

Based on the graph of Figure 10, it can be seen that contact pressure on the dimple surface is smaller than the surface without a dimple. This is indicated by the value of contact pressure at loading time of 0.12 seconds for the surface with a dimple is 0.407 Pa and the surface without dimple is 0.459 Pa. Smaller contact pressures can cause a positive outcome to improve lubrication performance. This is because the hydrodynamic pressure can provide a greater hydrodynamic lift force on a smaller contact pressure surface so as to increase the lubricant film thickness.

Based on the graph in Figure 11, it can be seen that the thickness of the lubricant layer of the surface on dimple is slightly greater than the surface without a dimple. This is indicated by the film thickness value on load condition ends at 1 second for the surface of the dimple is 22.692  $\mu\text{m}$  and the surface without dimple is 22.496  $\mu\text{m}$ . The lubricant film thickness film is one of the lubricating performance parameters, where the thicker the layer of the lubricant has the ability to withstand the given load.

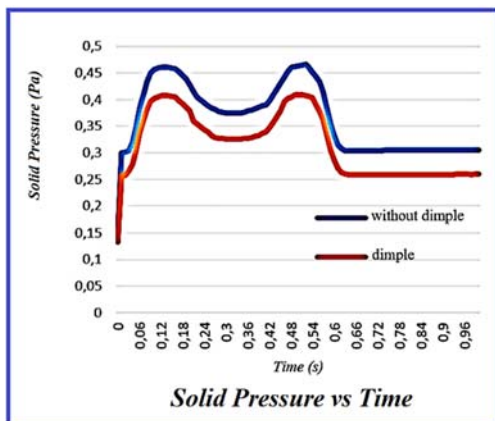


**Figure 10.** Comparison of solid pressure on surface dimple and without a dimple.

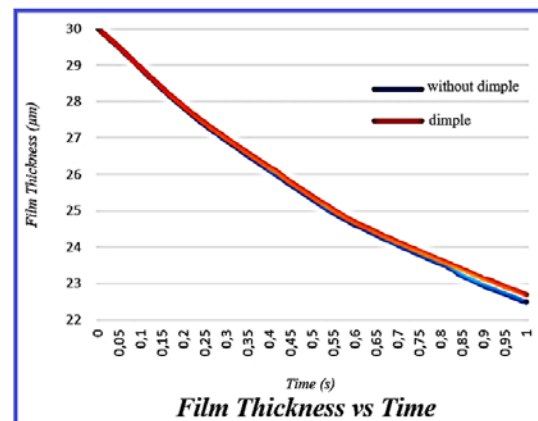


**Figure 11.** Comparison of film thickness lubricant on surface dimple and without a dimple.

It can be concluded that the dimple surface has a large hydrodynamic pressure and a small contact pressure, and the minimum lubricant thickness is of 22.692  $\mu\text{m}$ . On the surface without dimple has a value inversely proportional to the dimpled surface, the smaller the hydrodynamic pressure the greater contact pressure, where the minimum film thickness is 22.496  $\mu\text{m}$ . Thus it is an indication of good lubrication performance of the surface with a dimple.

The effect of quantity and pitch dimple of hydrodynamic pressure, it takes in 3 fixed variables of the dimple pitch 100  $\mu\text{m}$ , 300  $\mu\text{m}$ , and 500  $\mu\text{m}$  and with the dimple number of 3 dimples, 5 dimples, and 7 dimples.

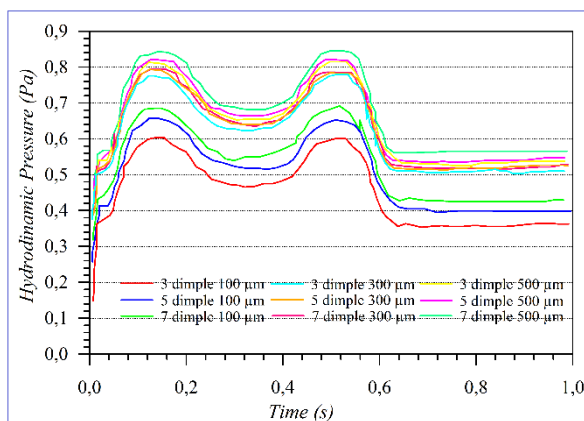


**Figure 12.** Comparison of hydrodynamic pressure between number and pitch of dimples.

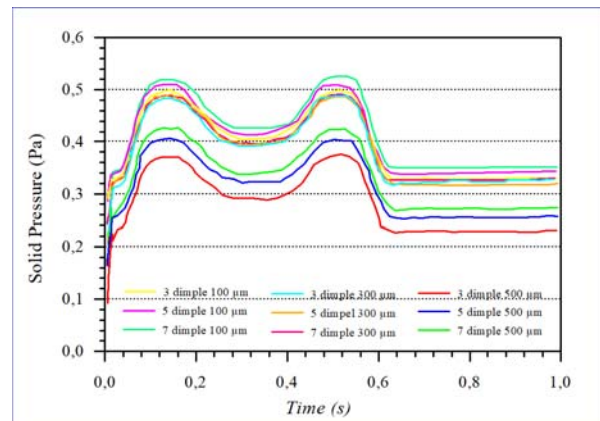


**Figure 13.** Comparison of contact pressure between number and pitch of dimples.

Based on the graph in Figure 12, showed that the effect of the increasing number of dimples will generate a pressure greater fluid hydrodynamics. Good lubrication performance is evidenced by large hydrodynamic pressures which have been investigated by [31,38]. The variation of 7 dimples has the greatest hydrodynamic pressure among other variations. This suggests that a variation of 7 dimples has the most effective potential to improve the performance of lubrication.

While the effect of dimple pitch of the hydrodynamic pressure is indicated in Figure 12. It can be determined that the increasing of dimple pitch of 100  $\mu\text{m}$ , 300  $\mu\text{m}$ , and 500  $\mu\text{m}$  will result in the increasing of the hydrodynamic pressure. Good lubrication performance is demonstrated by large hydrodynamic pressures, this has been investigated by [31,38]. The 500  $\mu\text{m}$  pitch variation has the greatest hydrodynamic pressure among other variations. This makes the 500  $\mu\text{m}$  variation of the dimple pitch has the most effective lubrication performance.



The effect of the number and pitch of the dimples on the contact pressure with the number of dimples of 3 dimples, 5 dimples, and 7 dimples and 3 fixed variables of dimple pitch 100  $\mu\text{m}$ , 300  $\mu\text{m}$ , and 500  $\mu\text{m}$ .

The effect of the number and pitch dimple against the contact pressure is indicated in Figure 13. It can be seen that the more the number of dimples the greater the contact pressure. Good lubrication performance is indicated by pressure on small contact pressure, this has been investigated by [38,39]. Although the contact pressure is greater than the increasing number of the dimple, the contact pressure does not exceed the hydrodynamic pressure of the fluid. The 3 dimples variation has the smallest contact pressure, while the 7 dimples variation has the greatest contact pressure.

The effect of a pitch dimple on the contact pressure is shown in Figure 13. It can be seen that the bigger the dimple pitch, the smaller the contact pressure that occurs. Good lubrication performance is presented by low contact pressure, this has been investigated by [39,40]. Pressure on low solid results in differences with larger hydrodynamic pressures, so the hydrodynamic pressure has the ability to increase the film thickness of the lubricant. The 500  $\mu\text{m}$  of dimple pitch variation has the lowest contact pressure among other variations.

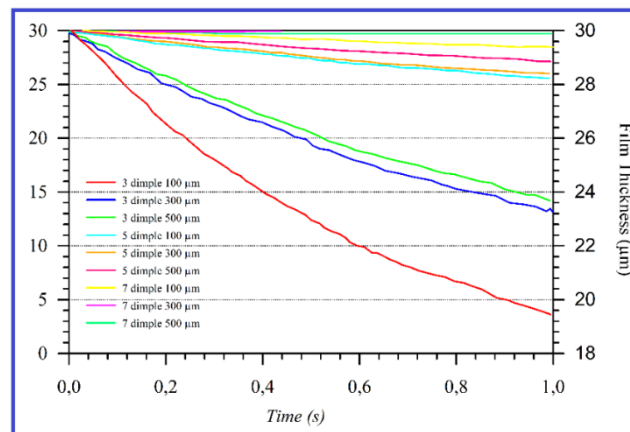


**Figure 14.** Comparison of film thickness between the variation of number and pitch dimple.

Based on the graph of the effect of the number and pitch of dimples on the film thickness is shown in Figure 14. It can be concluded that the greater the pitch of dimples will increase the film thickness of the lubricant. The increase in film thickness has a value that is directly proportional to the increased of hydrodynamic pressure and decreased the contact pressure. The 500  $\mu\text{m}$  pitch variation shows the highest lubricant film thickness, as it has been made by [17,33,41] which tells that the lubricant performance indicator is good by increasing film lubricating thickness.

Comparison of the number and a pitch dimple on the film thickness of the lubricant is shown in Figure 14. It can be concluded that an increase in the thickness of the lubricating film is caused by a larger number of the dimple. Improved the film thickness has a value that is directly proportional to the increased of hydrodynamic pressure. A large number of dimples mean that the number of the dimples will act as a reservoir of lubricants. The variation of 7 dimples has the highest lubricant film thickness among other variations.

#### 4. Conclusions

From the results and discussion of computer simulation which have been done can be drawn some conclusions as follows:

1. In the simulation method of CSM, under the dry condition, the addition of surface with dimples has a positive effect to reduce the contact pressure and indirectly reduce wear. This is evidence that the maximum surface contact pressure is 54.84 MPa with dimple and 94.22 MPa without a dimple.
2. In the simulation method of FSI, under the lubrication condition on the surface with and without dimple indicates that the hydrodynamic pressure is large and the contact pressure of solid is small, respectively. This will improve the lubricant film thickness, which is the lubrication performance

parameter. This is evidence that the hydrodynamic pressure on the surface of the dimple is 0.70 Pa, the contact pressure is 0.41 Pa, and the film thickness is 22.70  $\mu\text{m}$ .

3. In the FSI method, under the lubrication condition, the variation of 7 dimples and 500  $\mu\text{m}$  of dimple pitch is the best lubrication performance. The hydrodynamic pressure is 0.73 Pa, the contact pressure is 0.42 Pa, and the film thickness is 29.59  $\mu\text{m}$ . The increase of film thickness that occurs due to hydrodynamic pressure will cause the fluid lift force to withstand the loading of the solid structure.

## References

- [1] G Green, M Khan and F S Haddad 2015 Why do total hip replacements fail *Orthop. Trauma* **29** (2) 79–85
- [2] L Gao, F Wang, P Yang and Z Jin 2009 Effect of 3D physiological loading and motion on elastohydrodynamic lubrication of MoM total hip replacements *Med. Eng. Phys.* **31** (6) 720–729
- [3] B Sagbas and M N Durakbasa 2014 Surface texturing of vitamin e blended UHMWPE for reduction of wear *Acta Phys. Pol. A* **125** (2) 481–483
- [4] J Daniel, P B Pynsent and D J W McMinn 2004 MoM resurfacing of the hip in patients under the age of 55 years with osteoarthritis *J. Bone Joint Surg. Br.* **86B** (2) 177–184
- [5] I Etsion, Y Kligerman, and G Halperin 2008 Analytical and experimental investigation of laser-textured mechanical seal faces *Tribol. Trans.* **42** (3) 511–516
- [6] S R Brown, W A Davies, D H Deheer and A B Swanson 2002 Long-term survival of McKee-Farrar total hip prostheses (402) 157–163
- [7] A K Madl, M Liang, M Kovoichich, B L Finley, D J Paustenbach and G Oberdörster 2015 Toxicology of wear particles of cobalt-chromium alloy MoM hip implants Part I: Physicochemical properties inpatient and simulator studies *Nanomedicine Nanotechnology Biol. Med.* **11** (5) 1201–15
- [8] M Oldenburg, R Wegner, and X Baur 2009 Case report severe cobalt intoxication due to prosthesis wear in repeated total hip arthroplasty *J. Arthroplasty* **24** (5) 825.e15–e20
- [9] T Ss 2010 Arthroprosthetic cobaltism: neurological (Case 1) 2847–51
- [10] F D Adda 1994 Cardiac function study in hard metal workers **150** (93) 179–186
- [11] P Seghizzi, F D Adda, D Borleri, F Barbic, and G Mosconi 1994 Cobalt myocardiopathy a critical review of the literature **150** 105–109
- [12] G M Keegan, I D Learmonth and C P Case 2007 Orthopaedic metals and their potential toxicity in the arthroplasty patient: A review of current knowledge and future strategies *J. Bone Joint Surg. Br.* **89** (5) 567–573
- [13] D McMinn and J Daniel 2006 History and modern concepts in surface replacement *Proc. Inst. Mech. Eng. H.* **220** (2) 239–251
- [14] D Dowson and Z M Jin 2006 MoM hip joint tribology *Proc. Inst. Mech. Eng. Part H J. Eng. Med.* **220** (2) 107–118
- [15] I Etsion 2013 Modeling of surface texturing in hydrodynamic lubrication *Friction* **1** (3) 195–209
- [16] I Etsion 2004 Improving tribological performance of mechanical components by laser surface texturing **17** (4)
- [17] A Chyr, M Qiu, J W Speltz, R L Jacobsen, A P Sanders and B Raeymaekers 2014 A patterned microtexture to reduce friction and increase the longevity of prosthetic hip joints *Wear* **315** (1–2) 51–57
- [18] D Choudhury, R Walker, T Roy, S Paul and R Mootanah 2013 Performance of honed surface profiles to artificial hip joints: an experimental investigation *Int. J. Precis. Eng. Manuf.* **14** (10) 1847–53
- [19] D Choudhury, R Walker, A Shirvani and R Mootanah 2013 The influence of honed surfaces on MoM hip joints *Tribol. Online* **8** (3) 195–202
- [20] Q Wang 2015 Study on effect of dimples on the friction of parallel surfaces under different sliding conditions

- [21] T Matsuno 2000 Reduction of polyethylene wear by concave dimples on the frictional surface in artificial hip joints *J. Arthroplasty* **15** (3) 332–338
- [22] H Sawano, S Warisawa and S Ishihara 2009 Study on the long life of artificial joints by investigating optimal sliding surface geometry for improvement in wear resistance *Precis. Eng.* **33** (4) 492–498
- [23] T Roy, D Choudhury, S Ghosh, A Bin Mamat and B P Murphy 2014 Improved friction and wear performance of micro dimpled ceramic-on-ceramic interface for hip joint arthroplasty *Ceram. Int.* **41** (1) 681–690
- [24] L Gao, P Yang, I Dymond, J Fisher and Z Jin 2010 Effect of surface texturing on the elastohydrodynamic lubrication analysis of MoM hip implants *Tribol. Int.* **43** (10) 1851–60
- [25] S Narendra 2005 Design of a dimpled femoral head in total hip replacement using elastohydrodynamic lubrication theory 5–6
- [26] L M Gao, Q E Meng, F Liu, J Fisher and Z M Jin 2010 The effect of aspherical geometry and surface texturing on the elastohydrodynamic lubrication of MoM hip prostheses under physiological loading and motions *Proc. Inst. Mech. Eng. Part C* **224** (12) 2627–36
- [27] Y L Zhang, X G Zhang and G Matsoukas 2015 Numerical study of surface texturing for improving tribological properties of ultra-high molecular weight polyethylene *Biosurface and Biotribology* **1** (4) 270–277
- [28] M S Uddin and Y W Liu 2016 Design and optimization of a new geometric texture shape for the enhancement of hydrodynamic lubrication performance of parallel slider surfaces *Biosurface and Biotribology* 1–11
- [29] H A N Jing, L Fang, S U N Jiapeng and G E Shirong 2010 Hydrodynamic lubrication of micro dimple textured surface using three-dimensional CFD *Tribol. Trans.* **53** (6) 860–870
- [30] F Sahlin, S B Glavatskih, T Almqvist and R Larsson 2005 Two-dimensional CFD-analysis of micro-patterned surfaces in hydrodynamic lubrication *J. Tribol. Asme* **127** (1) 96–102
- [31] F Wang and Z Jin 2008 Transient elastohydrodynamic lubrication of hip joint implant *J. Tribol.* **130** (1) 011007
- [32] Z M Jin, M Stone, E Ingham and J Fisher 2006 Biotribology *Curr. Orthop.*
- [33] Q Meng, J Wang, P Yang, Z Jin and J Fisher 2015 The lubrication performance of the ceramic-on-ceramic hip implant under starved conditions *J. Mech. Behav. Biomed. Mater.* **50** 70–76
- [34] H Basri, A Syahrom, A T Prakoso, D Wicaksono and M I Amarullah 2018 The analysis of dimple geometry on the artificial hip joint to the performance of lubrication *Symposium of Emerging Nuclear Technology and Engineering Novelty* (to be published)
- [35] H Yu, X Wang and F Zhou 2010 Geometric shape effects of surface texture on the generation of hydrodynamic pressure between conformal contacting surfaces *Tribol. Lett.* **37** (2) 123–130
- [36] M Qiu, B R Minson and B Raeymaekers 2012 The effect of texture shape on the friction coefficient and stiffness of gas-lubricated parallel slider bearings *Tribol. Int.* **67** (3) 278–288
- [37] T Ibatan, M S Uddin and M A K Chowdhury 2015 Recent development on surface texturing in enhancing the tribological performance of bearing sliders *Surf. Coatings Technol.* **272** 102–120
- [38] H Zhang, L G Qin, M Hua, G N Dong and K S Chin 2015 A tribological study of the petaloid surface texturing for Co-Cr-Mo alloy artificial joints *Appl. Surf. Sci.* **332** 557–564
- [39] Q Meng, L Gao, F Liu, P Yang, J Fisher, and Z Jin 2010 Contact mechanics and elastohydrodynamic lubrication in a novel MoM hip implant with an aspherical bearing surface *J. Biomech.* **43** (5) 849–857
- [40] U Pettersson and S Jacobson 2007 Textured surfaces for improved lubrication at high pressure and low sliding speed of roller/piston in hydraulic motors *Tribol. Int.* **40** (2) 355–359
- [41] L Mourier, D Mazuyer, A A Lubrecht and C Donnet 2006 Transient increase of film thickness in micro-textured EHL contacts *Tribol. Int.* **39** (12) 1745–56